Comparative postnatal histomorphogenesis of the mandible in wild and laboratory mice

Jessica Martínez-Vargas[a,*], Cayetana Martinez-Maza[b], Francesc Muñoz-Muñoz[a], Nuria Medarde[a], Hayat Lamrous[c], María José López-Fuster[d], Jorge Cubo[c], Jacint Ventura[a]

[a] *Departament de Biologia Animal, de Biologia Vegetal i d'Ecologia, Facultat de Biociències, Universitat Autònoma de Barcelona, Campus de Bellaterra, E-08193 Cerdanyola del Vallès, Spain*

[b] *Departamento de Paleobiología, Museo Nacional de Ciencias Naturales (CSIC), C/ José Gutiérrez Abascal 2, E-28006 Madrid, Spain*

[c] *Sorbonne Universités, UPMC Univ Paris 06, CNRS, Institut des Sciences de la Terre Paris (iSTeP), 4 place Jussieu, BC 19, F-75005 Paris, France*

[d] *Departament de Biologia Evolutiva, Ecologia i Ciències Ambientals and Institut de Recerca de la Biodiversitat (IRBio), Facultat de Biologia, Universitat de Barcelona, Av. Diagonal 645, E-08028 Barcelona, Spain*

* Corresponding author.

E-mail addresses: jessmv88@gmail.com (J. Martínez-Vargas), martinezmaza.cayetana@gmail.com (C. Martinez-Maza), Francesc.MunozM@uab.cat (F. Muñoz-Muñoz), nuria.estel@gmail.com (N. Medarde), hayat.lamrous@upmc.fr (H. Lamrous), marialopez@ub.edu (M.J. López-Fuster), jorge.cubo_garcia@upmc.fr (J. Cubo), Jacint.Ventura.Queija@uab.cat (J. Ventura).

Abstract

The coordinated activity of bone cells (i.e., osteoblasts and osteoclasts) during ontogeny underlies observed changes in bone growth rates (recorded in bone histology and bone microstructure) and bone remodeling patterns explaining the ontogenetic variation in bone size and shape. Histological cross-sections of the mandible in the C57BL/6J inbred mouse strain were recently examined in order to analyze the bone microstructure, as well as the directions and rates of bone growth according to the patterns of fluorescent labeling, with the aim of description of the early postnatal histomorphogenesis of this skeletal structure. Here we use the same approach to characterize the histomorphogenesis of the mandible in wild specimens of *Mus musculus domesticus*, from the second to the eighth week of postnatal life, for the first time. In addition, we assess the degree of similarity in this biological process between the wild specimens examined and the C57BL/6J laboratory strain. Bone microstructure data show that *Mus musculus domesticus* and the C57BL/6J strain differ in the temporospatial pattern of histological maturation of the mandible, which particularly precludes the support of mandibular organization into the alveolar region and the ascending ramus modules at the histological level in *Mus musculus domesticus*. The patterns of fluorescent labeling reveal that the mandible of the wild mice exhibits temporospatial differences in the remodeling pattern, as well as higher growth rates particularly after weaning, compared to the laboratory mice. Since the two mouse groups were reared under the same conditions, the dissimilarities found suggest the existence of differences between the groups in the genetic regulation of bone remodeling, probably as a result of their different genetic backgrounds. Despite the usual suitability of inbred mouse strains as model organisms, inferences from them to natural populations regarding bone growth should be made with caution.

Abbreviations: PW, postnatal week.

Keywords: bone histology; bone remodeling; mandibular growth; modularity; *Mus musculus*; postnatal ontogeny; wild populations

1. Introduction

Bone remodeling refers to changes in size and shape of vertebrate skeletal elements during postnatal ontogeny (Enlow and Hans, 1996). This mechanism involves the coordinated activity of two types of bone cells: osteoblasts and osteoclasts (Enlow, 1963; Bloom and Fawcett, 1994; Baron and Kneissel, 2013). Osteoblasts secrete and mineralize the organic bone matrix, mainly composed of collagen fibers, and finally get trapped inside cavities within this matrix called osteocytic lacunae, where they differentiate into osteocytes (Robling and Turner, 2009). Osteoclasts demineralize and reabsorb the organic bone matrix, leaving concavities in the resorption front of bones named Howship's lacunae (Gilbert, 2000). The realization of the final bone shape and size is determined by the genetic program of bone cells, either inherited (phylogenetic signal) or species-specific (autapomorphies); however, it is also influenced by epigenetic factors: mechanical loads exerted by muscles, as well as metabolic and hormonal factors (Atchley and Hall, 1991; Enlow and Hans, 1996; Cubo et al., 2005; Robling et al., 2006; Baron and Kneissel, 2013; Burr and Allen, 2013).

Bone growth by deposition of periosteal tissue slows down over postnatal ontogeny (Amprino, 1947). This is concomitant with a gradual transformation of the histological bone microstructure: fast bone deposition results in woven bone tissue, while parallel-fibered bone tissue and especially lamellar bone tissue result from slower bone deposition (Amprino, 1947; de Ricqlès, 1975; de Buffrénil and Pascal, 1984; Castanet et al., 2000; Currey, 2002; de Margerie et al., 2002). In addition to the analysis of bone microstructure, the labeling of bones with fluorochrome markers has long been applied to the histological study of the dynamics of bone growth in vertebrates (Harris, 1960; Frost, 1969; Rahn and Perren, 1971; Meunier, 1972, 1974; Pautke et al., 2005; van Gaalen et al., 2010). Shortly after their supply *in vivo*, these vital fluorescent dyes are naturally fixed to the active mineralization front of the growing bone tissue. As a result, fluorescent labels appear as lines in histological cross-sections under ultraviolet light, and these lines actually correspond to the outline of the bone tissue mineralizing front at the time of the fluorochrome fixation (Pautke et al., 2005; van Gaalen et al., 2010). This

methodology allows for calculation of periosteal bone deposition rates, and can inform about the lack of net bone growth resulting from bone resting or osteoclastic bone resorption (van Gaalen et al., 2010). The examination of bone microstructure, but also of the directions and rates of periosteal bone deposition from histological cross-sections, has enabled the study of the postnatal histomorphogenesis and growth of several skeletal elements in different vertebrate species, like the long bones in humans and the mandible in mice (Bang and Enlow, 1967; de Buffrénil and Pascal, 1984; de Margerie et al., 2002; Martinez-Maza et al., 2012; Gosman et al., 2013; Cambra-Moo et al., 2015).

The mandible of the house mouse (*Mus musculus*) is a bony structure that originates from the assemblage of several neural-crest-derived morphogenetic units, and represents a key model system for research on the development, morphology, function, and evolution of complex morphological structures (Atchley and Hall, 1991; Hall, 2003; Klingenberg et al., 2004; Renaud et al., 2010; Muñoz-Muñoz et al., 2011; Klingenberg and Navarro, 2012). The early postnatal histomorphogenesis of the mouse mandible was recently characterized in the classical inbred mouse strain C57BL/6J (Martinez-Maza et al., 2012). The inbred laboratory mouse strains are indisputably very valuable and widely-used models in biological research; not only because mice have a shorter genetic distance with respect to humans than other model organisms, but also because these strains provide a wide range of different genotypes and phenotypes (Beck et al., 2000; Wade et al., 2002; Wade and Daly, 2005). However, the genomes of most classical inbred mouse strains, including C57BL/6J, consist of a mixture of segments from three house mouse subspecies found in nature and thus do not represent any of these subspecies, although *Mus musculus domesticus* is pointed out as having had a major role in the origin of these genetic mosaics (Bishop et al., 1985; Bonhomme et al., 1987; Boursot et al., 1993; Silver, 1995; Beck, 2000; Wade et al., 2002; Wade and Daly, 2005; Frazer et al., 2007; Yang et al., 2007, 2011; Didion and Pardo-Manuel de Villena, 2013).

To date, it has not been assessed whether or, if so, how the postnatal histomorphogenesis of the mandible differs between the C57BL/6J strain and *M. musculus domesticus*. The aim of the

present study is to explore to what extent this biological process is similar between these two genetically different but closely related groups of mice. To this end, we first examine the histological characterization and growth dynamics of the mandible in an ontogenetic series from the 2nd to the 8th week of postnatal life of wild-derived specimens of *M. musculus domesticus*. Then, we compare our results with those obtained by Martinez-Maza et al. (2012) from the C57BL/6J mouse strain, since the two samples were reared under the same conditions.

2. Materials and methods

2.1. Sample

Ten pregnant wild females of the western European house mouse (*Mus musculus domesticus* Schwarz and Schwarz, 1943) were -captured live with Sherman traps between 2009 and 2014 in Castellar del Vallès, Castellfollit del Boix, Nulles, and Santa Perpètua de Mogoda (Northeastern Iberian Peninsula). In these localities, only populations of *M. musculus domesticus* with the standard karyotype (2n=40) have been recorded (Medarde et al., 2012). Animal collection permits were granted from the Departament d'Agricultura, Ramaderia, Pesca, Alimentació i Medi Natural of the Generalitat de Catalunya (Government of Catalonia; Catalonia, Spain). Each pregnant female was housed separately in a standard cage with environmental enrichment, and placed in an animal room under controlled conditions at Universitat Autònoma de Barcelona (Barcelona, Spain). Litters were born after a few days, and the day of birth of each one was noted. Animals were monitored daily, and supplied with water as well as food *ad libitum*.

To ensure their survival right after birth, the newborns were housed together with their biological mothers and were not manipulated during their first week of postnatal life. The sample used in this study consisted of 36 mouse pups that survived this critical period, and remained alive until euthanasia. The value of this sample is worth noting, since several critical points conditioned its acquisition. First, the live-trapping of evidently pregnant wild females; then, their accommodation to the laboratory conditions despite their high susceptibility to

stress; finally, the birth and survival of their pups during the entire process. After all, a sample size equivalent to that used by Martinez-Maza et al. (2012) was obtained.

In order to match the growth conditions between our mice and those analyzed by Martinez-Maza et al. (2012), each litter of wild mice was housed together with a foster mother of the C57BL/6J strain and her own pups from the 7th postnatal day. In each case, own and adoptive offspring of each wet-nurse female were about the same age. When the final litter sizes exceeded the average in normal conditions (6-8 pups), some of the biological pups were removed. The biological litters were not included in this study. In addition to being a standardizing measure, this fostering strategy was followed due to the better suitability of female mice from laboratory strains to breed in captivity; wild animals are more sensitive to stress in captive conditions and, therefore, stress affects more severely their breeding performance (Wallace, 1976). Water and the same diet supplied by Martinez-Maza et al. (2012) to their sample, consisting of standard rodent pellets, were supplied *ad libitum* in all cages. Thus, the two mouse groups under comparison were fed the same diet before and after weaning, a developmental milestone typically occurs around the 21st postnatal day that in the house mouse.

Mouse pups were allowed to grow until they were two to eight weeks old. Sample sizes were balanced according to weeks approximately as in Martinez-Maza et al. (2012): 2 weeks, n=6; 3 weeks, n=7; 4 weeks, n=7; 5 weeks, n=6; 6 weeks, n=4; 7 weeks, n=3; 8 weeks, n=3. Specimens were euthanized by cervical dislocation. Due to the existence of populations of *M. musculus domesticus* with Robertsonian translocations in Northeastern Iberian Peninsula (Medarde et al., 2012), all mice were karyotyped in order to avoid the potential inclusion of animals with this chromosomal rearrangement in our study. Karyotypes were obtained from marrow cells of the femurs and dyed with Wright stain (Ford, 1966; Mandahl, 1992). Chromosomes were identified under a light microscope (Nikon Eclipse 50i) according to the Committee on Standardized Genetic Nomenclature for Mice (1972). As expected, all specimens had the standard karyotype, and will be named “wild mice” hereafter. We will refer to the specimens of the C57BL/6J strain analyzed by Martinez-Maza et al. (2012) as “lab mice”.

2.2. Histological analyses of bone microstructure and growth dynamics

The characterization of the postnatal histomorphogenesis of the mandible in wild mice was approached through the analysis of its internal microstructure and growth dynamics (i.e., directions and rates of bone growth) from histological cross-sections, in accordance with Martinez-Maza et al. (2012). In order to examine and quantify the dynamics of bone growth, intraperitoneal injections of the fluorochrome Xylenol Orange (80 mg kg^{-1} of body weight, pH=7) were supplied *in vivo* to all specimens. As indicated by Rahn and Perren (1971), this fluorescent dye reacts in the same way the fluorochrome dicarboxymethyl aminomethyl fluorescein (DCAF), used by Martinez-Maza et al. (2012), does. Therefore, both dyes can be used indistinctly without having any consequence on the results; the only difference is that Xylenol Orange labels the bone in orange instead of green. Because of the relatively high mortality rate among mice of the C57BL/6J strain when a fluorescent dye was supplied right after birth (own data), all mice in the present study received the first injection of Xylenol Orange at the end of the 1st PW (i.e., 7th postnatal day). Injections were then administered weekly to each specimen, and ceased exactly one week before euthanasia (e.g., the 4-week-old specimens received three injections, specifically at the end of the 1st, 2nd, and 3rd PW, and were sacrificed one week after the last injection).

Mandibles were dissected; the left and right dentary bones were then separated at the mandibular symphysis and carefully cleaned by hand. The 36 right dentary bones were dehydrated in graded ethanol, defatted in trichloroethylene and acetone, dried at 38–40°C in a stove, and embedded in a polyester resin. Using a diamond-tipped circular saw, histological cross-sections of 100µm (± 10µm) thickness were obtained from four mandibular regions, following Martinez-Maza et al. (2012): diastema, first molar, second molar, and ascending ramus at the level of the condylar and angular processes (Fig. 1). After being ground and polished, each thin section was mounted on a slide. All the histological cross-sections were observed with an

inverted fluorescent microscope (Zeiss Axiovert 35), and photographed under natural light as well as ultraviolet light with a digital camera coupled to the microscope.

The pictures taken under natural light were examined to identify and map the spatial distribution of woven and parallel-fibered bone tissue in the different subregions of periosteal bone defined in each mandibular cross-section (Fig. 1). Woven bone tissue is characterized by collagen fibers with a low ordered spatial arrangement, and randomly distributed rounded osteocytic lacunae (Fig. 2). Parallel-fibered bone tissue shows a parallel arrangement of collagen fibers, and flattened osteocytic lacunae in an ordered disposition (Fig. 2). The distribution of these two types of bone tissue, observed in more than half of the specimens of the same age, was noted, which allowed us to establish a general histological pattern for each mandibular region in each PW.

The pictures taken under ultraviolet light were examined to determine the directions and rates of periosteal growth of the four mandibular regions throughout ontogeny, using a Xylenol Orange labeling. The presence in the periosteum of the fluorescent label corresponding to the last injection of fluorochrome, together with new non-labeled bone tissue added in its periphery, was associated with bone deposition during the last week of life (Fig. 3). The absence of the fluorescent label corresponding to the last injection could be associated either with bone resorption resulting from osteoclastic activity in the periosteal or endosteal bone surface (Fig. 3) (Enlow and Hans, 1996), or with resting bone (i.e., cessation of growth), during the last week of life. Because the local loss of fluorescent label from the endosteal bone surface was linked to periosteal bone deposition in the immediately surrounding areas, it was considered to result from osteoclastic activity instead of a resting bone surface. In order to identify the phenomenon responsible for the absence of fluorescent label from the periosteal bone surfaces, a histological analysis of the mandibular surfaces was conducted, bearing in mind that Howship's lacunae are a direct indicator of osteoclastic activity (Martinez-Maza et al., 2010). Following this method, we also supplemented the information regarding the processes underlying the absence of fluorescent labeling in lab mice (see Martinez-Maza et al., 2012) by using another ontogenetic

series of the C57BL/6J strain. Several subregions, according to sets of observation points, were established in the four mandibular regions to simplify the examinations of the labeling (Figs. 4–7). The patterns of presence and absence of fluorochrome detected in more than half of the specimens of the same age were noted, so that a general labeling pattern was established for each mandibular region in each PW.

When periosteal bone deposition occurred during the last week of life, periosteal growth rates were calculated. To this end, the distance between the most peripheral fluorescent label in the histological cross-sections, corresponding to the last injection of fluorochrome, and the periosteal bone surface was measured with the image processing package Fiji, a distribution of ImageJ (Schindelin et al., 2012). Measurements were taken at different points, which covered the whole outline of the histological cross-sections, following Martinez-Maza et al. (2012) (Figs. 4–7). An effort was made to assess and reduce measurement error, because it affects linear measurements and could lead to biased growth rates (Bailey and Byrnes, 1990). Following Rasmussen et al. (2001), inter-observer error was minimized by standardizing the measurements, and training the person who obtained them from the sample of wild mice (JMV) under the strict supervision of the person who performed them in the sample of lab mice (CMM). In order to evaluate intra-observer error, three replicates of all measurements were performed by the same person (JMV) in a subsample of ten individuals. A model II one-way ANOVA, with measurements as the dependent variables and 'individual' as the factor, was performed to test whether variation among individuals was higher than among replicates (Arnqvist and Martensson, 1998). Statistical significance was corrected with the sequential Bonferroni correction (Holm, 1979; Rice, 1989). Because variation among individuals significantly exceeded variation among replicates ($P<0.01$ in all measurements), intra-observer measurement error was considered negligible and measurements were obtained once from all individuals by the same person (JMV). Daily rates of periosteal bone growth (μm day^{-1}) corresponding to the last week of life were obtained dividing the distances by 7 (i.e., the number of days elapsed between the last fluorochrome injection and euthanasia). Adjacent measurement points showing similar

growth rates along ontogeny were grouped, which led to the delimitation of different subregions in each mandibular region as in Martinez-Maza et al. (2012) (Figs. 4–7). The mean periosteal growth rate of each mandibular subregion was calculated for each specimen, by averaging the growth rates corresponding to the measurement points comprised, even if bone deposition was not the only or main activity detected. The mean growth rates of each subregion were then further averaged among the specimens of the same age, and the standard deviations for the mean values were obtained.

Mean bone growth rates of all mandibular subregions were compared between wild and lab mice of the same age. The values corresponding to the sample of lab mice studied by Martinez Maza et al. (2012) were recalculated from raw data available. Given that the Shapiro-Wilk W test revealed that data generally deviated significantly from a normal distribution ($P<0.05$), the non-parametric Mann-Whitney U test was used for the comparisons. Statistical significance was subjected to sequential Bonferroni correction (Holm, 1979; Rice, 1989).

3. Results

3.1. Mandibular microstructure

Wild mice exhibited woven bone tissue alone in the dorsal and ventral parts of the diastema, in the lingual side of the two molar regions, as well as in the labial side of the condylar process, during the whole study period. This histological pattern was also found in the labial and ventral sides of the two molar regions, as well as in the lingual side of the condylar process, between the 2nd and 5th PW, and in the ventral ascending ramus from the 2nd to the 4th PW (Table 1). Parallel-fibered and woven bone tissues were found together from the 2nd PW in the lingual side of the diastema, and from the 5th PW onwards in the labial side of the diastema and the ventral ascending ramus. From the 6th PW, both tissue types were also detected in the labial and ventral sides of the first molar region, as well as in the lingual side of the condylar process (Table 1). The histological results corresponding to lab mice can be found in Table 1 within Martinez-Maza et

al. (2012). The differences detected between the two mouse groups under comparison are summarized in the following subsections.

3.1.1. Diastema region

Although the two groups generally showed both types of bone tissue in the labial side over ontogeny, the presence of woven or parallel-fibered bone alone had a different timing in each group. In the lingual side, wild mice exhibited woven bone in its dorsal half and parallel-fibered bone in its ventral half most of the time, while lab mice displayed parallel-fibered bone alone especially from the 6th PW onwards.

3.1.2. First molar region

Wild mice exhibited a central area of parallel-fibered bone surrounded by woven bone, in the labial and ventral sides, from the 6th PW onwards. From the 3rd PW, lab mice displayed parallel-fibered and woven bone respectively in the dorsal and ventral halves of the labial side, and only parallel-fibered bone in the lingual side. Woven bone was found in the ventral area of lab mice most of the time.

3.1.3. Second molar region

In wild mice from the 7th and 8th PW, the labial side displayed a central area of parallel-fibered bone surrounded by woven bone. In lab mice, the labial side exhibited parallel-fibered and woven bone respectively in the dorsal and ventral halves from the 4th PW. Only lab mice exhibited parallel-fibered bone in the lingual side from the 4th PW.

3.1.4. Ascending ramus region

Wild mice from the 5th PW onwards showed woven bone surrounding a central area of parallel-fibered bone in the ventral ascending ramus, while lab mice started displaying both

types of bone tissue in this region from the 6th PW. The condylar tip began to exhibit the two types of bone tissue in the 6th PW in wild mice, but in the 8th PW in lab mice.

3.2. Mandibular growth dynamics

Endosteal bone resorption in wild mice was detected during the initial weeks in the diastema and the two molar regions. Instead, periosteal bone resorption was more evident towards the end of the study period, particularly in the molars alveoli and the ventral half of the ascending ramus (Table 2, and Figs. 4–7 for the visualization of the mandibular subregions). The mean rates of periosteal bone growth in all mandibular regions of wild mice were relatively higher at the beginning of the study period than towards its end (Table 3, Figs. 4–7). The original results corresponding to lab mice can be found in Figs. 4–5 and within the text in Martinez-Maza et al. (2012), but are also represented here in the same format as those of wild mice (Tables 3 and 4, Figs. 4–7). A summarized comparison between the two groups is provided in the subsections below.

3.2.1. Diastema region

Endosteal bone resorption in wild mice was observed in the ventral half of the labial side and the ventral area (points 6-8 and 9-11) from the 2nd to the 4th PW, but just until the 3rd PW in the ventro-lingual area (points 9-14) of lab mice (Tables 2 and 4). Absence of fluorescent labeling was detected in the dorsal area (points 1-3) and dorsal half of the lingual side (points 15-18) of wild mice between the 6th and 8th PW, but only in the latter region in lab mice from the 4th PW onwards (Tables 2 and 4). Resting bone surface seemed to be responsible for this pattern, as no Howship's lacunae were detected.

Diastema growth accelerated more evidently in wild mice in the 3rd PW, while it suddenly slowed in the 4th PW and gradually decelerated afterwards in both groups. The ventro-labial area (points 6-11) grew at a comparatively greater speed in both groups, particularly during the initial weeks (Fig. 4, Table 3). Wild mice exhibited significantly (P<0.05) higher mean growth

rates in the lingual side (points 12-18) during most of the study period, and in the ventro-labial area in the 8th PW (Fig. 4, Table 3).

3.2.2. First molar region

Endosteal bone resorption was detected in the whole ventral half (points 6-14) of wild mice just during the 2nd PW, but in the ventro-lingual area (points 9-14) of lab mice until the 3rd PW (Tables 2 and 4). Periosteal bone resorption was identified in the dorsal half of the lingual side (points 15-17) from the 5th and 6th PW onwards in wild and lab mice, respectively. Absence of fluorescent labeling in this region was also observed in wild mice between the 2nd and 4th PW, likely due to resting bone, as well as in lab mice from the 3rd to the 5th PW, although in this case the cause could not be ascertained (Tables 2 and 4).

Growth of the first molar region slowed down gradually over ontogeny in both groups, although some subregions occasionally showed slight growth accelerations, like the ventral and lingual sides (points 9-11 and 12-17) of wild mice in the 3rd PW. Bone growth rates of the ventro-labial area (points 6-8 and 9-11) were comparatively higher over ontogeny in both groups (Fig. 5, Table 3). The mean growth rates of the lingual side (points 12-17) were usually significantly greater among wild mice ($P<0.05$; Fig. 5, Table 3).

3.2.3. Second molar region

Endosteal bone resorption in wild mice was detected above the mandibular crest of the labial side (points 4-5) and in the ventral area (points 8-10) just during the 2nd PW, while in lab mice it was observed in the ventro-lingual area (points 8-12) until the 3rd PW (Tables 2 and 4). Periosteal bone resorption was observed in the dorsal half of the lingual side (points 13-14) in wild and lab mice, from the 5th and 6th PW onwards respectively. This remodeling activity was also identified in the dorsal half of the labial side (points 1-3) of wild mice during the whole study period (Tables 2 and 4).

An increase in the growth rate of the whole second molar region in wild mice, but of its ventral area (points 6-10) in lab mice, was detected in the 3rd PW. Growth deceleration in the 4th PW was steeper in wild mice, and a gradual growth slowdown was observed in both groups thereafter. The ventral area grew comparatively faster over ontogeny in both groups (Fig. 6, Table 3). The mean growth rates of the labial and lingual sides (points 1-5 and 11-14) were often significantly higher in wild mice (P<0.05). The ventral area grew significantly faster in lab mice in the 5th PW, but in wild mice, in the 7th PW (P<0.05; Fig. 6, Table 3).

3.2.4. Ascending ramus region

Absence of fluorescent label from the periosteal bone surface, of unknown cause, was detected in the labial side of the condylar tip (points 1-3) in both groups from the 4th PW onwards, and in its lingual side (points 17-20) only in wild mice from the 5th PW (Tables 2 and 4). The lingual side of the ventral half of the ramus (points 12-16) displayed periosteal bone resorption from the 6th PW onwards in wild mice, but from the 4th PW in lab mice. In the 6th and 8th PW, only wild mice exhibited periosteal bone resorption in the labial side of the ventral half of the ramus (points 6-9) (Tables 2 and 4).

The analysis of the bone growth rates was constrained by the limited fluorescent labeling. Bone deposition rates generally increased in the 3rd PW, and a sudden growth slowdown in the 4th PW was followed by a gradual growth deceleration, in both mouse groups (Fig. 7, Table 3). Apart from the lingual side of the condylar tip (points 17-20), all subregions grew significantly faster (P<0.05) among wild mice in several weeks (Fig. 7, Table 3).

4. Discussion

4.1. Bone remodeling and dynamics of mandibular growth

The patterns of fluorescent labeling revealed that the wild and lab mice under comparison exhibited endosteal bone resorption, together with relatively fast periosteal bone deposition, in the ventral half of the diastema and of both molar regions at the beginning of the study period.

The combination of these two remodeling activities indicated a prominent downward growth of the anterior mandibular region in both groups. Different gene regulatory networks have been suggested to underlie mandibular growth and dental development. Nonetheless, these two processes must be synchronized in order to guarantee the functional viability of the mandible and teeth (Fraser et al., 2009; Paradis et al., 2013). The eruption of the effective adult mouse dentition (i.e., incisors and the first two pairs of molars) is complete around the 21st postnatal day (Swiderski and Zelditch, 2013). Furthermore, tooth roots are generated later than crowns, and roots formation chronologically coincides with dental eruption (Jheon et al., 2013). Therefore, the increase in height, by ventral bone drift, of the diastema as well as the first and second molar regions would be expected to last until the end of the 3rd PW in the house mouse. Indeed, the lab mice analyzed by Martinez-Maza et al. (2012) displayed ventral cortical drift in the anterior region of the mandible up to the end of the 3rd PW. Thus, in that case the above mentioned spatio-temporal synchronization between dental development and mandibular remodeling is supported, as also observed in other works with inbred mouse strains (Lungová et al., 2011; Swiderski and Zelditch, 2013). Instead, the wild mice analyzed in the present study did not show evident ventral drift of the molar region beyond the 2nd PW, although their diastema underwent notable ventral growth until the 4th PW. These between-group differences in the timing of remodeling of the distal part of the mandible suggest between-group differences in the timing of tooth development. Particularly, our results indicate that molar development might be more accelerated in wild mice, compared to lab mice. When qualitatively analyzing the pattern of dental eruption in the sample of wild mice used in the present study and in a different ontogenetic series of the C57BL/6J strain from the 2nd to the 8th PW, eruption of the molars and incisors appeared to be slightly faster among wild mice. In particular, a relatively greater portion of the molars and incisors crowns had emerged through the alveolar bone in wild mice both in the 2nd and 3rd PW. Nevertheless, tooth eruption appeared to be complete in both mouse groups by the 4th PW (own data available under request). Therefore, these patterns of dental development seem to be congruent with the remodeling patterns of the molar region detected

and compared in this study. However, the different timing of eruption of the incisors does not seem to explain the between-group differences in the remodeling of the diastema region. In that case, and bearing in mind that mouse incisors show horizontal position and continuous growth throughout life, it might be that the incisors were relatively thicker in wild mice. If so, the ventral cortical drift of the diastema should indeed last longer in wild mice for the mandible to host the incisor roots. However, some other reasons may also explain the differences in the remodeling pattern of the diastema observed between the two groups, which would require further investigation.

Deposition and resorption activities in bone surface respectively face and oppose the direction of bone growth (Enlow and Hans, 1996). Also, even slight changes in bone deposition rates can result in notable differences in the final size and shape of bones (Robling et al., 2003). Therefore, the uneven distribution of the two remodeling activities, together with the differences in the speed of growth, detected in the different regions of the mouse mandible over ontogeny are very likely to contribute to the ontogenetic morphological variation of this bony structure (Robinson and Sarnat, 1955; Bang and Enlow, 1967). The wild and lab mice under comparison differed in the specific timing and spatial distribution of both periosteal and endosteal bone resorption activities in each mandibular region. Furthermore, periosteal bone deposition particularly in the labial and lingual surfaces of the mandible tended to be significantly faster in wild mice from the 3rd PW onwards, which suggests a greater widening and, thus, robustness of the dentary bone in *M. musculus domesticus* after weaning. Therefore, these between-group dissimilarities in mandibular remodeling, resulting in evident between-group differences in the directions and magnitude of mandibular growth, would likely account to some extent for between-group variation in mandibular morphology. Accordingly, the recent detection of variation in mandibular growth and form between *M. musculus domesticus* and the C57BL/6J strain during early postnatal ontogeny, through bone surface and geometric morphometric analyses, indeed pointed to differences in the remodeling process, probably of genetic nature, as a possible causing factor (Martínez-Vargas et al., 2017).

The presence of periosteal resorption in the molar region was restricted to the molar alveoli in both groups of mice. However, while the spatial pattern of this remodeling activity would result in the lateral displacement of molar alveoli in lab mice, it would result in the narrowing of this mandibular region in wild mice. Given that molar eruption was complete by the time these resorption patterns were noticed, the displacement, but especially the narrowing of the molar alveoli, could be aimed at fitting the mandible to the lesser width of the molar roots, compared to the molar crowns. This notion seems to be supported by the fact that the above mentioned remodeling pattern was detected earlier in the molar region of wild mice, bearing in mind that, as stated, molar development appeared to be faster in wild mice than in lab mice.

Periosteal bone resorption in the ascending ramus appeared to be restricted to its ventral half in both mouse groups, since the cause behind the absence of fluorescent labeling in the condylar tip could not be ascertained. Nevertheless, different growth directions of this mandibular region could be deduced in each group. In wild mice, the condylar tip stopped growing on its labial side in the 4th PW, and stopped widening from the 5th PW onwards, while the ventral part of the ramus narrowed from the 6th PW. Instead, lab mice displayed medial growth at the condylar tip and lateral growth of the ventral part of the ramus since the 4th PW, which implied a vertical arrangement of this mandibular region (Martinez-Maza et al., 2012). Despite these between-group differences in the remodeling pattern of the ascending ramus, both wild and lab mice lacked fluorescent labeling in this mandibular region from the 4th PW onwards, that is to say, after weaning. Given that weaning implies a shift towards a solid diet, it also means the onset of active gnawing and chewing. As a result, the fiber properties of the masticatory muscles change, and the mechanical load on the mandible, but especially on the ascending ramus, increases (Shida et al., 2005; Suzuki et al., 2007). The deformation of the bone matrix caused by the local tissue strains is detected by mechanosensors, which foster bone deposition or resorption depending on whether the muscular loading respectively exceeds a certain threshold or not (Robling et al., 2006; Robling and Turner, 2009; Enomoto et al., 2010; Baron and Kneissel, 2013; Burr and Allen, 2013). Accordingly, the notable change in the

remodeling pattern of the ascending ramus in both mouse groups after the 4th PW could be the reflection of the response of this mandibular region to the new post-weaning mechanical loads. Although muscular loading might be expected to increase after weaning, the presence of bone resorption activity may be reflecting the fact that probably not all masticatory muscles promote post-weaning bone deposition in this mandibular region (Herring, 2011).

4.2. Relationship between bone growth and bone microstructure

The comprehensive interpretation of both the examinations of bone tissue types and the quantifications of periosteal bone growth in the mandible of *M. musculus domesticus* indicates that our results support Amprino's rule (1947), as happened with the lab mice analyzed by Martinez-Maza et al. (2012). The temporal succession from woven to parallel-fibered bone tissue was observed, since the proportion of woven bone tissue was greater during the first few weeks and parallel-fibered bone tissue was more extensive by the end of the study period. Furthermore, the relationship between bone growth rate and bone tissue type established in Amprino's rule (1947) was detected, since the highest growth rates were observed during the initial weeks of postnatal growth. Likewise, growth rates over ontogeny were relatively higher in the mandibular areas that retained woven bone tissue. The observation of the ranges of growth rates associated with each histological pattern revealed that the upper threshold was higher when only woven bone tissue was deposited, compared to when parallel-fibered bone tissue was also present. However, the lower threshold happened to be quite the same regardless of the histological characterization. Therefore, the ranges of growth rates ascribed to each histological pattern were wide and overlapped between them, in agreement with previous observations (Castanet et al., 2000; de Margerie et al., 2002, 2004; Starck and Chinsamy, 2002). Consequently, the present work supports that histological characterization of bones might not always be an unequivocal predictor of bone deposition rates, and that therefore Amprino's rule should be carefully considered, as also suggested by prior studies (Castanet et al., 2000; de Margerie et al., 2002, 2004; Starck and Chinsamy, 2002). Nevertheless, the fact that *M. musculus domesticus* and

the C57BL/6J mouse strain showed similar ranges of growth rates associated with each histological pattern suggests that the relationship between bone microstructure and the speed of bone deposition is quite conserved between these two mouse groups.

4.3. Temporospatial pattern of histological maturation

The fact that the histological transformation from woven to parallel-fibered bone tissue over ontogeny is correlated with a certain slowdown in bone growth makes this histological change to be regarded as a reflection of bone maturation (de Ricqlès, 1975; Currey, 2002). The shift from woven to parallel-fibered bone in the C57BL/6J mouse strain took place first in the diastema and the two molar regions, and later in the ascending ramus region. This temporospatial difference in the histological characterization of the mandible suggested a distinct developmental pattern between its anterior and posterior regions (Martinez-Maza et al., 2012). As a result, this finding was interpreted as supporting the modular organization of the mouse mandible into the alveolar region (bearing the teeth) and the ascending ramus (serving as the main attachment region for masticatory muscles) from a histological point of view (Martinez-Maza et al., 2012), in accordance with previous studies with developmental or covariational focuses (Atchley and Hall, 1991; Klingenberg et al., 2003; Muñoz-Muñoz et al., 2011; Burgio et al., 2012). Unlike in the laboratory mouse strain, in *M. musculus domesticus* the histological patterns of bone maturation of the diastema and the two molar regions were found to be asynchronic, whereas synchrony was detected between both molar regions and the ascending ramus region. Therefore, under the same rationale of results interpretation for the C57BL/6J strain, the timing of histological maturation of the different regions of the mandible in *M. musculus domesticus* during early postnatal ontogeny would not support the abovementioned modular organization at the histological level. However, in both mouse groups the sampling of mandibular sections was relatively limited. Particularly, the histological sampling of the ascending ramus region was sparse compared to that of the distal part of the mandible. Therefore, this fact precludes an accurate assessment of synchrony in the patterns of histological

maturation among the different subregions of the ascending ramus region, and across the entire mandible. Consequently, this limitation restricts the distinction among different hypotheses of modularity, and therefore cautions against making strong statements about the existence or inexistence of any kind of histological modularity in the mouse mandible. The assessment of which hypothesis of modularity, if any, might be validated in each mouse group at the histological level would likely require a more thorough sampling of mandibular sections in future studies. Nevertheless, the results of the present work reveal that, following the protocol established by Martinez-Maza et al. (2012), the temporospatial pattern of histological maturation of the mandible actually differs between the C57BL/6J strain and *M. musculus domesticus*. Despite this discrepancy, the temporal pattern of change from immature (woven) to more mature (parallel-fibered) bone tissue seemed to follow an anteroposterior gradient in both mouse groups, which suggests that the polarity of mandibular maturation might be also conserved between *M. musculus domesticus* and the C57BL/6J strain. Again, though, a more exhaustive sampling of mandibular sections would be needed in order to validate this notion.

5. Conclusions

The present study provides evidence that the histomorphogenesis of the mandible during early postnatal life differs to some extent between natural populations of *M. musculus domesticus* and the C57BL/6J inbred laboratory strain. Particularly, these two mouse groups differ in the directions, timing, and rates of growth, as well as in the spatiotemporal pattern of distribution of bone tissue types, characterizing early postnatal mandibular development. However, the link between bone microstructure and the speed of bone deposition, together with the anteroposterior gradient of histological maturation of the mandible, appear to be common features to both mouse groups. Bearing in mind the equivalent growth conditions of the wild and laboratory mice under comparison, the dissimilarities detected between their patterns of mandibular histomorphogenesis likely result from the inherent genetic differentiation between the two groups. Their distinct genomic constitutions might have resulted in variation in the

genetic regulation of mandibular remodeling and dental development, as well as probably in differences in bone sensitivity to perceive mechanical stimuli and in bone ability to transform these stimuli into responses from bone cells (see Judex et al., 2002; Robling and Turner, 2002, 2009). The differences here reported caution against the over-extrapolation of results from laboratory animals to natural populations, particularly regarding the patterns of postnatal bone growth.

Author contributions

Conception and design of the study: JV, CMM, JC, MJLF. Acquisition of data: JMV, HL, NM, MJLF. Data analysis and interpretation: JMV, CMM. Drafting of the manuscript: JMV. Critical revision of the manuscript: JV, JC, FMM, CMM. All authors read and approved the final manuscript.

Ethical consideration

The protocol followed in the present study was approved by the Comissió d'Ètica en l'Experimentació Animal i Humana (CEEAH) of the Universitat Autònoma de Barcelona, and by the Departament d'Agricultura, Ramaderia, Pesca, Alimentació i Medi Natural (Direcció General de Medi Natural i Biodiversitat) of the Generalitat de Catalunya (Permit Number: DAAM 6328). Animal handling strictly accorded with the guidelines approved by these entities.

Conflicts of interest

None.

Acknowledgments

This work was supported by the Spanish Ministerio de Economía y Competitividad (grant number CGL2010-15243, to JV), and the Generalitat de Catalunya (grant number 2014-SGR-1241). JMV received a PIF fellowship from the Universitat Autònoma de Barcelona. The funding

sources had no involvement in study design; in the collection, analysis, and interpretation of data; in the writing of the report; nor in the decision to submit the article for publication. This study was conducted in the framework of the PhD program in Biodiversity from Universitat Autònoma de Barcelona.

References

Amprino, R., 1947. La structure du tissu osseux envisagée comme expression de différences dans la vitesse de l'accroissement. Arch. Biol. 58, 315–330.

Arnqvist, G., Martensson, T., 1998. Measurement error in geometric morphometrics: empirical strategies to assess and reduce its impact on measures of shape. Acta. Zool. Academ. Sci. Hung. 44, 73–96.

Atchley, W.R., Hall, B., 1991. A model for development and evolution of complex morphological structures. Biol. Rev. Camb. Philos. Soc. 66, 101–157.

Bailey, R.C., Byrnes, J., 1990. A new, old method for assessing measurement error in both univariate and multivariate morphometrics studies. Syst. Zool. 39, 124–130.

Bang, S., Enlow, D.H., 1967. Postnatal growth of the rabbit mandible. Arch. Oral Biol. 12, 993–998.

Baron, R., Kneissel, M., 2013. WNT signaling in bone homeostasis and disease: from human mutations to treatments. Nat. Med. 19, 179–192.

Beck, J.A., Lloyd, S., Hafezparast, M., Lennon-Pierce, M., Eppig, J.T., Festing, M.F., Fisher, E.M., 2000. Genealogies of mouse inbred strains. Nat. Genet. 24, 23–25.

Bishop, C.E., Boursot, P., Baron, B., Bonhomme, F., Hatat, D., 1985. Most classical *Mus musculus domesticus* laboratory mouse strains carry a *Mus musculus musculus* Y chromosome. Nature 315, 70–72.

Bloom, W., Fawcett, D.W., 1994. A Textbook of Histology, 12th ed. Chapman & Hall, New York.

Bonhomme, F., Guénet, J.-L., Dod, B., Moriwaki, K., Bulfield, G., 1987. The polyphyletic origin of laboratory inbred mice and their rate of evolution. Biol. J. Linn. Soc. Lond. 30, 51–58.

Boursot, P., Auffray, J.-C., Britton-Davidian, J., Bonhomme, F., 1993. The evolution of house mice. Annu. Rev. Ecol. Syst. 24, 119–152.

Burgio, G., Baylac, M., Heyer, E., Montagutelli, X., 2012. Exploration of the genetic organization of morphological modularity on the mouse mandible using a set of interspecific recombinant congenic strains between C57BL/6 and mice of the *Mus spretus* species. G3 2, 1257–1268.

Burr, D.B., Allen, M.R., 2013. Basic and Applied Bone Biology, 1st ed. Academic Press, Amsterdam.

Cambra-Moo, O., Nacarino-Meneses, C., Díaz-Güemes, I., Enciso, S., García Gil, O., Llorente Rodríguez, L., Rodríguez Barbero, M.Á., de Aza, A.H., González Martín, A., 2015. Multidisciplinary characterization of the long-bone cortex growth patterns through sheep's ontogeny. J. Struct. Biol. 191, 1–9.

Castanet, J., Rogers, K.C., Cubo, J., Boisard, J.J., 2000. Periosteal bone growth rates in extant ratites (ostriche and emu). Implications for assessing growth in dinosaurs. C. R. Acad. Sci. III, Sci. Vie 323, 543–550.

Committee on Standardized Genetic Nomenclature for Mice, 1972. Standard karyotype of the mouse, *Mus musculus*. Heredity 63, 69–72.

Cubo, J., Ponton, F., Laurin, M., de Margerie, E., Castanet, J., 2005. Phylogenetic signal in bone microstructure of sauropsids. Syst. Biol. 54, 562–574.

Currey, J.D., 2002. Bones: Structure and Mechanics, 1st ed. Princeton University Press, New Jersey.

de Buffrénil, V., Pascal, M., 1984. Croissance et morphogénèse postnatales de la mandibule du vison (*Mustela vison* Schreiber): données sur la dynamique et l'interprétation fonctionnelle des dépôts osseux mandibulaires. Can. J. Zool. 62, 2026–2037.

de Margerie, E., Cubo, J., Castanet, J., 2002. Bone typology and growth rate: testing and quantifying 'Amprino's rule' in the mallard (*Anas platyrhynchos*). C. R. Biol. 325, 221–230.

de Margerie, E., Robin, J.P., Verrier, D., Cubo, J., Groscolas, R., Castanet, J., 2004. Assessing a relationship between bone microstructure and growth rate: a fluorescent labelling study in the king penguin chick (*Aptenodytes patagonicus*). J. Exp. Biol. 207, 869–879.

de Ricqlès, A., 1975. Recherches paléohistologiques sur les os longs des tétrapodes. VII- Sur la classification, la signification fonctionnelle et l'histoire des tissus osseux de tétrapodes (Première partie: Structures). Ann. Paléontol. 61, 51–129.

Didion, J.P., Pardo-Manuel de Villena, F., 2013. Deconstructing *Mus gemischus*: advances in understanding ancestry, structure, and variation in the genome of the laboratory mouse. Mamm. Genome 24, 1–20.

Enlow, D.H., 1963. Principles of Bone Remodeling: An Account of Post-Natal Growth and Remodeling Process in Long Bone and the Mandible, 1st ed. Charles C. Thomas, Springfield.

Enlow, D.H., Hans, M.G., 1996. Essentials of Facial Growth, 1st ed. WB Saunders, Philadelphia.

Enomoto, A., Watahiki, J., Yamaguchi, T., Irie, T., Tachikawa, T., Maki, K., 2010. Effects of mastication on mandibular growth evaluated by microcomputed tomography. Eur. J. Orthod. 32, 66–70.

Ford, C.E., 1966. The use of chromosome markers. In: Micklem, H.S., Loutit, J.F. (Eds.). Tissue Grafting and Radiation. Academic Press, New York, pp. 197–206.

Fraser, G.J., Hulsey, C.D., Bloomquist, R.F., Uyesugi, K., Manley, N.R., Streelman, J.T., 2009. An ancient gene network is co-opted for teeth on old and new jaws. PLoS Biol. 7, e1000031.

Frazer, K.A., Eskin, E., Kang, H.M., Bogue, M.A., Hinds, D.A., Beilharz, E.J., Gupta, R.V., Montgomery, J., Morenzoni, M.M., Nilsen, G.B., Pethiyagoda, C.L., Stuve, L.L., Johnson, F.M., Daly, M.J., Wade, C.M., Cox, D.R., 2007. A sequence-based variation map of 8.27 million SNPs in inbred mouse strains. Nature 448, 1050–1053.

Frost, H.M., 1969. Tetracycline-based histological analysis of bone remodeling. Calcif. Tissue Res. 3, 211–237.

Gilbert, S.F., 2000. Developmental Biology, 6th ed. Sinauer Associates, Sunderland.

Gosman, J.H., Hubbell, Z.R., Shaw, C.N., Ryan, T.M., 2013. Development of cortical bone geometry in the human femoral and tibial diaphysis. Anat. Rec. 296, 774–787.

Hall, B.K., 2003. Unlocking the black box between genotype and phenotype. Cell condensations as morphogenetic (modular units). Biol. Philos. 18, 219–247.

Harris, W.H., 1960. A microscopic method of determining rates of bone growth. Nature 188, 1038–1039.

Herring, S.W., 2011. Muscle-bone interactions and the development of skeletal phenotype: jaw muscles and the skull. In: Hallgrimsson, B., Hall, B.K. (Eds.). Epigenetics: Linking Genotype and Phenotype in Development and Evolution. University of California Press, Berkley, pp. 221–237.

Holm, S., 1979. A simple sequentially rejective multiple test procedure. Scand. J. Statist. 6, 65–70.

Jheon, A.H., Seidel, K., Biehs, B., Klein, O.D., 2013. From molecules to mastication: the development and evolution of teeth. Wiley Interdiscip. Rev. Dev. Biol. 2, 165–182.

Judex, S., Donahue, L.R., Rubin, C., 2002. Genetic predisposition to low bone mass is paralleled by an enhanced sensitivity to signals anabolic to the skeleton. FASEB J. 16, 1280–1282.

Klingenberg, C.P., Navarro, N., 2012. Development of the mouse mandible: a model system for complex morphological structures. In: Macholán, M., Baird, S.J.E., Munclinger, P., Piálek, J. (Eds.). Evolution of the House Mouse. Cambridge University Press, Cambridge, pp. 135–149.

Klingenberg, C.P., Mebus, K., Auffray, J.C., 2003. Developmental integration in a complex morphological structure: how distinct are the modules in the mouse mandible? Evol. Dev. 5, 522–531.

Klingenberg, C.P., Leamy, L.J., Cheverud, J.M., 2004. Integration and modularity of quantitative trait locus effects on geometric shape in the mouse mandible. Genetics 166, 1909–1921.

Lungová, V., Radlanski, R.J., Tucker, A.S., Renz, H., Míšek, I., Matalová, E., 2011. Tooth-bone morphogenesis during postnatal stages of mouse first molar development. J. Anat. 218, 699–716.

Mandahl, N., 1992. Methods in solid tumor cytogenetics. In: Rooney, D.E., Czepulkowski, B.H. (Eds.). Human Cytogenetics. A Practical Approach. IRL Press, London, pp. 155–187.

Martinez-Maza, C., Rosas, A., Nieto-Diaz, M., 2010. Brief communication: identification of bone formation and resorption surfaces by reflected light microscopy. Am. J. Phys. Anthropol. 143, 313–320.

Martinez-Maza, C., Montes, L., Lamrous, H., Ventura, J., Cubo, J., 2012. Postnatal histomorphogenesis of the mandible in the house mouse. J. Anat. 220, 472–483.

Martínez-Vargas, J., Muñoz-Muñoz, F., Martinez-Maza, C., Molinero, A., Ventura, J., 2017. Postnatal mandible growth in wild and laboratory mice: differences revealed from bone remodeling patterns and geometric morphometrics. J. Morphol. (*in press*). DOI: 10.1002/jmor.20694.

Medarde, N., López-Fuster, M.J., Muñoz-Muñoz, F., Ventura, J., 2012. Spatio-temporal variation in the structure of a chromosomal polymorphism zone in the house mouse. Heredity 109, 78–89.

Meunier, F., 1972. Marquages simples et multiples du tissu osseux de quelques Téléostéens par des substances fluorescentes. C. R. Acad. Sci. 275, 1685–1688.

Meunier, F., 1974. La technique de marquage vital des tissus squelettiques des poissons. Bull. Fr. Piscic. 255, 51–57.

Muñoz-Muñoz, F., Sans-Fuentes, M.A., López-Fuster, M.J., Ventura, J., 2011. Evolutionary modularity of the mouse mandible: dissecting the effect of chromosomal reorganizations and isolation by distance in a Robertsonian system of *Mus musculus domesticus*. J. Evol. Biol. 24, 1763–1776.

Paradis, M.R., Raj, M.T., Boughner, J.C., 2013. Jaw growth in the absence of teeth: the developmental morphology of edentulous mandibles using the p63 mouse mutant. Evol. Dev. 15, 268–279.

Pautke, C., Vogt, S., Tischer, T., Wexel, G., Deppe, H., Milz, S., Schieker, M., Kolk, A., 2005. Polychrome labeling of bone with seven different fluorochromes: enhancing fluorochrome discrimination by spectral image analysis. Bone 37, 441–445.

Rahn, B.A., Perren, S.M., 1971. Xylenol orange, a fluorochrome useful in polychrome sequential labeling of calcifying tissues. Stain Technol. 46, 125–129.

Rasmussen, P.W., Wheeler, W.E., Moser, T.J., Vine, L.E., Sullivan, B.D., Rusch, D.H., 2001. Measurements of Canada goose morphology: sources of error and effects on classification of subspecies. J. Wildl. Manage. 65, 716–725.

Renaud, S., Auffray, J.-C., de la Porte, S., 2010. Epigenetic effects on the mouse mandible: common features and discrepancies in remodeling due to muscular dystrophy and response to food consistency. BMC Evol. Biol. 10, 28.

Rice, W.R., 1989. Analyzing tables of statistical tests. Evolution 43, 223–225.

Robinson, I.B., Sarnat, B.G., 1955. Growth pattern of the pig mandible; a serial roentgenographic study using metallic implants. Am. J. Anat. 96, 37–64.

Robling, A.G., Turner, C.H., 2002. Mechanotransduction in bone: genetic effects on mechanosensitivity in mice. Bone 31, 562–569.

Robling, A.G., Turner, C.H., 2009. Mechanical signaling for bone modeling and remodeling. Crit. Rev. Eukaryot. Gene Expr. 19, 319–338.

Robling, A.G., Li, J., Shultz, K.L., Beamer, W.G., Turner, C.H., 2003. Evidence for a skeletal mechanosensitivity gene on mouse chromosome 4. FASEB J. 17, 324–326.

Robling, A.G., Castillo, A.B., Turner, C.H., 2006. Biomechanical and molecular regulation of bone remodeling. Annu. Rev. Biomed. Eng. 8, 455–498.

Schindelin, J., Arganda-Carreras, I., Frise, E., Kaynig, V., Longair, M., Pietzsch, T., Preibisch, S., Rueden, C., Saalfeld, S., Schmid, B., Tinevez, J.Y., White, D.J., Hartenstein, V., Eliceiri, K., Tomancak, P., Cardona, A., 2012. Fiji: an open-source platform for biological-image analysis. Nat. Methods 9, 676–682.

Schwarz, E., Schwarz, H.K., 1943. The wild and commensal stocks of the house mouse, *Mus musculus* Linnaeus. J. Mammal. 24, 59–72.

Shida, T., Abe, S., Sakiyama, K., Agematsu, H., Mitarashi, S., Tamatsu, Y., Ide, Y., 2005. Superficial and deep layer muscle fibre properties of the mouse masseter before and after weaning. Arch. Oral Biol. 50, 65–71.

Silver, L.M., 1995. Mouse Genetics: Concepts and Applications, 1st ed. Oxford University Press, New York.

Starck, J.M., Chinsamy, A., 2002. Bone microstructure and developmental plasticity in birds and other dinosaurs. J. Morphol. 254, 232–246.

Suzuki, K., Abe, S., Kim, H.J., Usami, A., Iwanuma, O., Okubo, H., Ide, Y., 2007. Changes in the muscle fibre properties of the mouse temporal muscle after weaning. Anat. Histol. Embryol. 36, 103–106.

Swiderski, D.L., Zelditch, M.L., 2013. The complex ontogenetic trajectory of mandibular shape in a laboratory mouse. J. Anat. 223, 568–580.

van Gaalen, S.M., Kruyt, M.C., Geuze, R.E., de Bruijn, J.D., Alblas, J., Dhert, W.J., 2010. Use of fluorochrome labels in *in vivo* bone tissue engineering research. Tissue Eng. Part B, Rev. 16, 209–217.

Wade, C.M., Kulbokas III, E.J., Kirby, A.W., Zody, M.C., Mullikin, J.C., Lander, E.S., Lindblad-Toh, K., Daly, M.J., 2002. The mosaic structure of variation in the laboratory mouse genome. Nature 420, 574–578.

Wade, C.M., Daly, M.J., 2005. Genetic variation in laboratory mice. Nat. Genet. 37, 1175–1180.

Wallace, M., 1976. Effects of stress due to deprivation and transport in different genotypes of house mouse. Lab. Anim. 10, 335–347.

Yang, H., Bell, T.A., Churchill, G.A., Pardo-Manuel de Villena, F., 2007. On the subspecific origin of the laboratory mouse. Nat. Genet. 39, 1100–1107.

Yang, H., Wang, J.R., Didion, J.P., Buus, R.J., Bell, T.A., Welsh, C.E., Bonhomme, F., Hon-Tsen Yu, A., Nachman, M.W., Piálek, J., Tucker, P., Boursot, P., McMillan, L., Churchill, G.A., Pardo-Manuel de Villena, F., 2011. Subspecific origin and haplotype diversity in the laboratory mouse. Nat. Genet. 43, 648–655.

Figure captions

Fig. 1. Localization seen from the lingual side (top) and appearance under natural light (bottom) of the histological cross-sections of the *Mus musculus domesticus* mandible: (A) diastema region; (B) first molar region; (C) second molar region; (D) ascending ramus region at the level of the condylar and angular processes. Upper scale bar: 5mm; lower scale bar: 1mm.

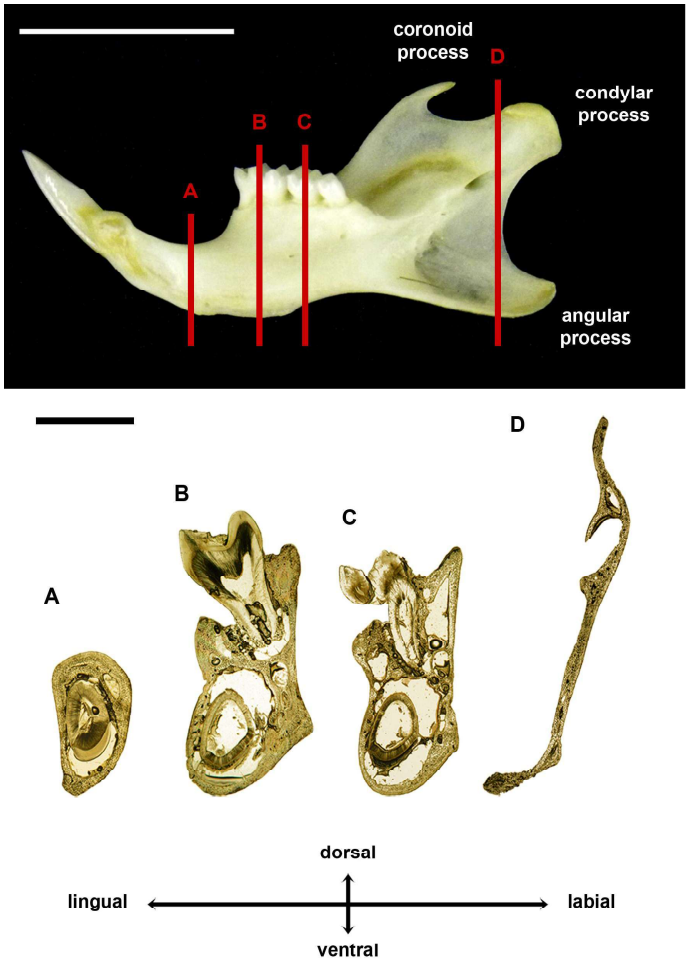

Fig. 2. Bone tissue types identified in the histological cross-sections of the mandible of *Mus musculus domesticus*: (A) woven bone tissue; (B) parallel-fibered bone tissue. Scale bars: 100μm.

Fig. 3. Patterns of fluorescent labeling resulting from bone deposition and resorption activities. The presence of fluorescent label in the periosteal region and accretion of bone tissue in its periphery evidences periosteal bone deposition. The absence of fluorescent label due to bone resorption can occur from the endosteal (left) and periosteal (right) bone surfaces. Scale bar: 1mm.

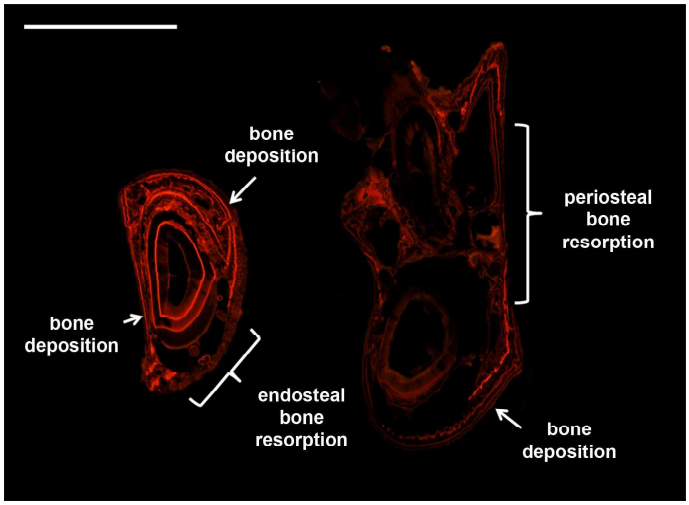

Fig. 4. Histological cross-section of the diastema region under ultraviolet light with the measurement points (left), and periosteal bone growth rates (mean ± standard deviation, in μm day^{-1}) of its different subregions in each postnatal week (right): (A) dorsal region and dorsal half of the labial side (points 1-5); (B) ventral half of the labial side and ventral region (points 6-11); (C) lingual side (points 12-18). BGR = bone growth rate. Scale bar: 1mm. Numerical values are displayed in Table 3.

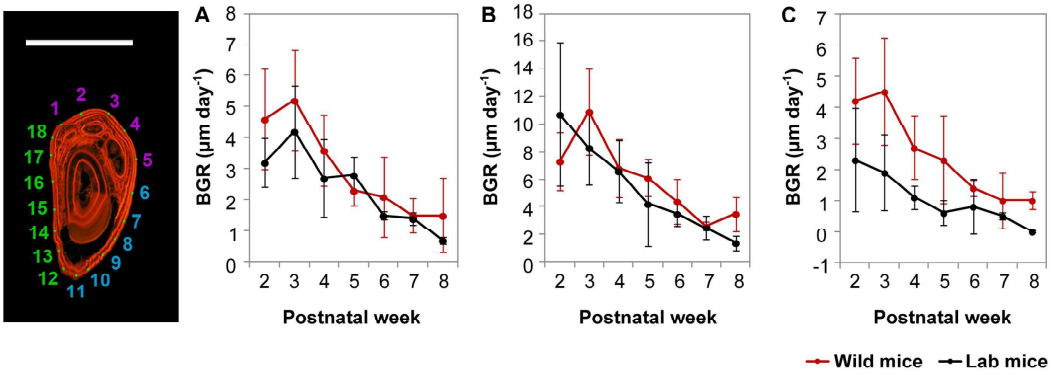

Fig. 5. Histological cross-section of the first molar region under ultraviolet light with the measurement points (left), and periosteal bone growth rates (mean ± standard deviation, in μm day^{-1}) of its different subregions in each postnatal week (right): (A) dorsal half of the labial side (points 1-5); (B) ventral half of the labial side (points 6-8); (C) ventral region (points 9-11); (D) lingual side (points 12-17). BGR = bone growth rate. Scale bar: 1mm. Numerical values are displayed in Table 3.

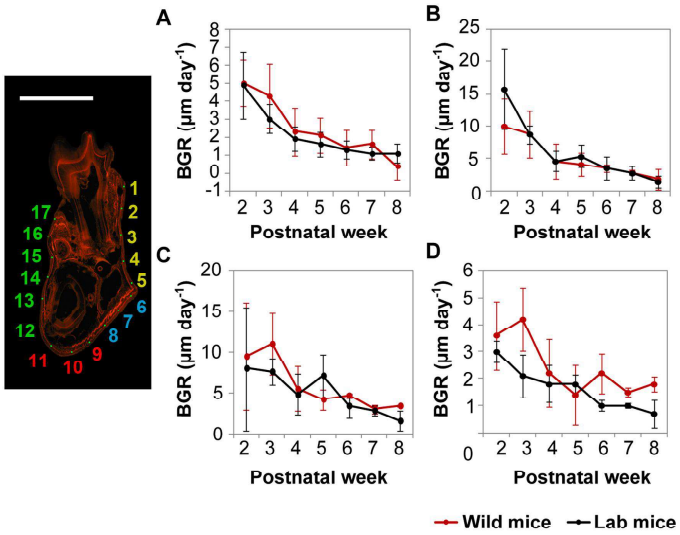

Fig. 6. Histological cross-section of the second molar region under ultraviolet light with the measurement points (left), and periosteal bone growth rates (mean ± standard deviation, in μm day^{-1}) of its different subregions in each postnatal week (right): (A) labial side (points 1-5); (B) ventral region (points 6-10); (C) lingual side (points 11-14). BGR = bone growth rate. Scale bar: 1mm. Numerical values are displayed in Table 3.

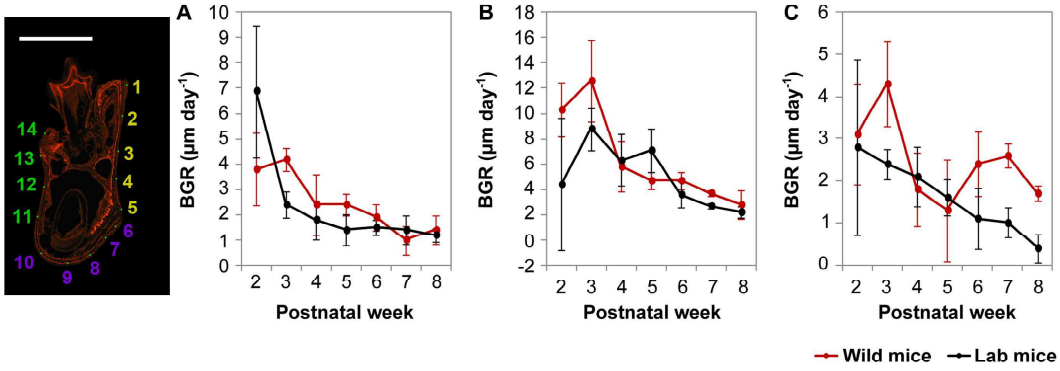

Fig. 7. Histological cross-section of the ascending ramus region at the level of the condylar and angular processes under ultraviolet light with the measurement points (left), and periosteal bone growth rates (mean ± standard deviation, in μm day^{-1}) of its different subregions in each postnatal week (right): (A) labial side of the condylar process (points 1-3); (B) labial side of the ventral part (points 4-9); (C) ventral region of the angular process (points 10-11); (D) lingual side of the ventral part (points 12-16); (E) lingual side of the condylar process (points 17-20). BGR = bone growth rate. Scale bar: 1mm. Numerical values are displayed in Table 3.

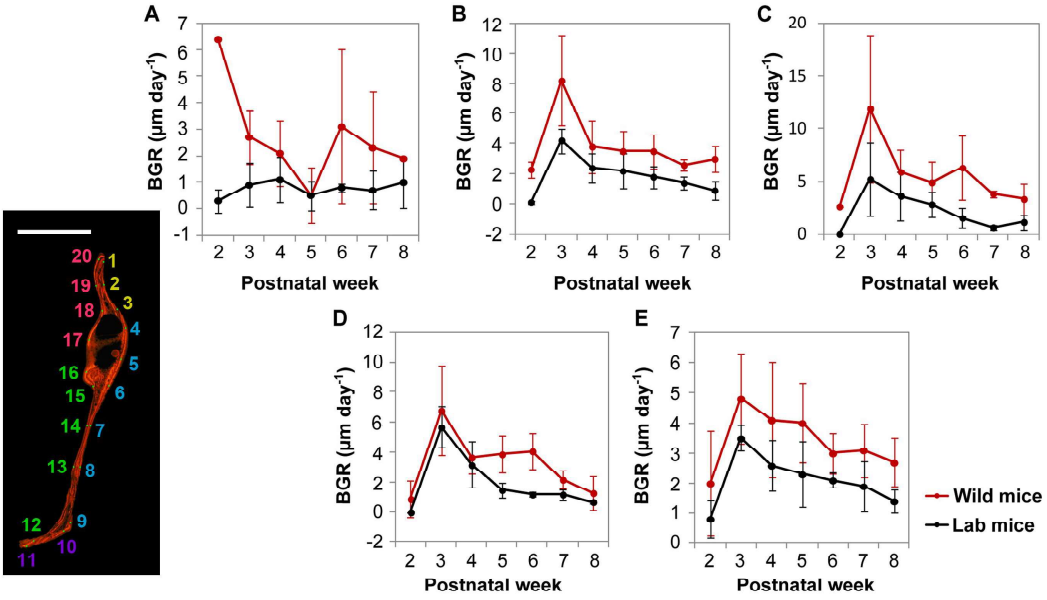

Table 1

Distribution of bone tissue types most frequently observed in the mandible of wild mice in each postnatal week.

PW	n	Mandible region and subregion																
		Diastema					First molar				Second molar				Ascending ramus			
		dor	lab	ven	lin		lab	ven	lin		lab	ven	lin		C lab	C lin	V lab	V lin
2nd	6	w	w/pf/w	w	pf/w		w	w	w		w	w	w		w	w	w	w
3rd	7	w	w	w	pf/w		w	w	w		w	w	w		w	w	w	w
4th	7	w	w	w	pf/w		w	w	w		w	w	w		w	w	w	w
5th	6	w	pf/w	w	pf/w		w	w	w		w	w	w		w	w	w/pf/w	w/pf/w
6th	4	w	pf/w	w	pf/w		w/pf/w	w/pf/w	w		w	pf/w	w		w	w/pf/w	w/pf/w	w/pf/w
7th	3	w	w/pf/w	w	w		w/pf/w	w/pf/w	w		w/pf/w	w	w		w	w/pf/w	w/pf/w	w/pf/w
8th	3	w	w/pf/w	w	pf/w		w/pf/w	w/pf/w	w		w/pf/w	w	w		w	w/pf/w	w/pf/w	w/pf/w

PW: postnatal week; n: sample size; dor: dorsal; lab: labial; ven: ventral; lin: lingual; C lab: labial side of the condylar process; C lin: lingual side of the condylar process; V lab: labial side of the ventral half; V lin: lingual side of the ventral half; w: woven bone tissue; pf: parallel-fibered bone tissue; pf/w – w/pf/w: woven and parallel-fibered bone tissues observed in the same region, clockwise.

Table 2

Pattern of presence and absence of Xylenol Orange labeling most frequently observed in each mandible region, subregion, and postnatal week among wild mice.

Mandible region	Mandible subregion	Postnatal week						
		2nd	3rd	4th	5th	6th	7th	8th
Diastema	1-3							
	4-5							
	6-8							
	9-11							
	12-14							
	15-18							
First molar	1-3							
	4-5							
	6-8							
	9-11							
	12-14							
	15-17							
Second molar	1-3							
	4-5							
	6-7							
	8-10							
	11-12							
	13-14							
Ascending ramus	1-3							
	4-5							
	6-9							
	10-11							
	12-16							
	17-20							

White: presence of fluorescent labeling, indicating bone deposition; *black*: absence of fluorescent labeling, likely due to periosteal bone resorption; *gray*: absence of fluorescent labeling, likely due to endosteal bone resorption; *black and white stripes*: absence of fluorescent labeling, likely due to resting bone; *black and white grid*: absence of fluorescent labeling, unknown cause. Mandible subregions are set based on the localization of the points used to calculate the bone growth rates (see Figs. 4–7).

Table 3

Periosteal bone growth rates (mean ± standard deviation, in μm day^{-1}) of the mandible of wild and laboratory mice along ontogeny. For each postnatal week, upper row corresponds to wild mice and lower row to lab mice.

PW	n	Mandible region and subregion														
		Diastema			First molar				Second molar			Ascending ramus				
		1-5	6-11	12-18	1-5	6-8	9-11	12-17	1-5	6-10	11-14	1-3	4-9	10-11	12-16	17-20
2nd	6	4.6±1.6	7.3±2.1	4.2±1.4	5.0±1.3	10.0±4.3	9.5±6.6	3.6±1.3	3.8±1.4	10.3±2.1	3.1±1.2	6.4±0.0	2.3±0.6	2.6±0.0	0.9±1.2	2.0±1.8
	6	3.2±0.8	10.7±5.2	2.3±1.7	4.9±1.9	15.7±6.2	8.0±7.6	3.0±0.4	6.9±2.6	4.4±5.2	2.8±2.1	0.3±0.4	0.1±0.1	0.0±0.0	0.0±0.0	0.8±0.6
3rd	7	5.2±1.6	10.9±3.1	**4.5±1.7***	4.3±1.8	8.7±3.6	11.0±3.8	**4.2±1.2***	**4.2±0.5***	12.6±3.2	**4.3±1.0***	**2.7±1.0***	**8.2±3.0***	11.9±7.0	6.8±3.0	4.8±1.5
	6	4.2±1.5	8.3±2.7	**1.9±1.2***	3.0±0.8	8.7±1.4	7.6±1.6	**2.1±0.8***	**2.4±0.5***	8.8±1.7	**2.4±0.3***	**0.9±0.9***	**4.2±0.8***	5.2±3.5	5.7±1.3	3.5±0.4
4th	7	3.6±1.2	6.8±2.1	**2.7±1.0***	2.3±1.3	4.6±2.7	5.5±2.7	2.2±1.3	2.4±1.2	5.8±2.0	1.8±0.9	2.1±1.2	3.8±1.7	5.9±2.1	3.7±1.1	4.1±1.9
	8	2.7±1.3	6.6±2.3	**1.1±0.4***	1.9±0.7	4.6±1.5	4.8±2.5	1.8±0.7	1.8±0.8	6.3±2.0	2.1±0.7	1.1±0.9	2.4±0.9	3.6±2.3	3.2±1.5	2.6±0.8
5th	6	2.3±0.5	6.1±1.3	**2.3±1.4***	2.1±1.0	4.1±1.8	4.2±1.3	1.4±1.1	**2.4±0.4***	**4.7±0.7***	1.3±1.2	0.5±1.1	3.5±1.3	4.9±2.0	**3.9±1.2***	4.0±1.3
	6	2.8±0.6	4.2±3.0	**0.6±0.4***	1.6±0.7	5.3±1.7	7.1±2.6	1.8±0.3	**1.4±0.6***	**7.1±1.7***	1.6±0.4	0.5±0.6	2.2±1.2	2.8±1.2	**1.5±0.5***	2.3±1.1
6th	4	2.1±1.3	4.4±1.6	1.4±0.2	1.4±1.0	3.5±0.6	4.7±0.3	**2.2±0.7***	1.9±0.5	4.7±0.7	2.4±0.8	3.1±2.9	3.5±1.1	**6.3±3.0***	**4.1±1.2***	3.0±0.7
	4	1.5±0.1	3.5±0.9	0.8±0.9	1.3±0.5	3.5±1.8	3.4±1.4	**1.0±0.2***	1.5±0.3	3.6±1.0	1.1±0.7	0.8±0.2	1.8±0.7	**1.5±0.9***	**1.2±0.2***	2.1±0.2
7th	3	1.5±0.5	2.6±0.3	1.0±0.9	1.6±0.8	2.8±0.4	3.0±0.6	**1.5±0.2***	1.0±0.6	**3.7±0.2***	**2.6±0.3***	2.3±2.1	**2.6±0.4***	**3.8±0.4***	**2.2±0.6***	3.1±0.9

		3		1.4 ±0.2	2.5± 0.8	0.5± 0.1		1.1 ±0.3	2.7± 1.1	2.8± 0.6	**1.0± 0.1***		1.4± 0.6	**2.7± 0.2***	**1.0± 0.4***		0.7± 0.7	**1.4± 0.4***	**0.6± 0.3***	**1.2± 0.3***	1.9 ±0.8
8th		3		1.5 ±1.2	**3.5± 1.2***	**1.0± 0.3***		0.4 ±0.7	1.8± 1.6	3.4± 0.1	1.8± 0.3		1.4± 0.6	2.8± 1.1	1.7± 0.2		1.9± 0.0	3.0± 0.8	3.3± 1.5	1.3± 1.2	2.7 ±0.8
		3		0.7 ±0.1	**1.4± 0.5***	**0.0± 0.0***		1.1 ±0.5	1.4± 0.8	1.6± 1.2	0.7± 0.5		1.2± 0.3	2.2± 0.5	0.4± 0.4		1.0± 1.0	0.9± 0.6	1.1± 0.7	0.7± 0.1	1.4 ±0.4

*Bone growth rates significantly different between wild and lab mice (Mann-Whitney U test and sequential Bonferroni correction, $P<0.05$). PW: postnatal week; n: sample size. Mandible subregions (number ranges) are set based on the localization of the points used to calculate the bone growth rates (see Figs. 4–7).

Table 4

Pattern of presence and absence of Xylenol Orange labeling most frequently observed in each mandible region, subregion, and postnatal week among lab mice.

Mandible region	Mandible subregion	Postnatal week						
		2nd	3rd	4th	5th	6th	7th	8th
Diastema	1-3							
	4-5							
	6-8							
	9-11							
	12-14							
	15-18							
First molar	1-3							
	4-5							
	6-8							
	9-11							
	12-14							
	15-17							
Second molar	1-3							
	4-5							
	6-7							
	8-10							
	11-12							
	13-14							
Ascending ramus	1-3							
	4-5							
	6-9							
	10-11							
	12-16							
	17-20							

White: presence of fluorescent labeling, indicating bone deposition; *black*: absence of fluorescent labeling, likely due to periosteal bone resorption; *gray*: absence of fluorescent labeling, likely due to endosteal bone resorption; *black and white stripes*: absence of fluorescent labeling, likely due to resting bone; *black and white grid*: absence of fluorescent labeling, unknown cause. Mandible subregions are set based on the localization of the points used to calculate the bone growth rates (see Figs. 4–7).